Evolution of solar flare SOL 2013-05-17: analysis of optical spectra (Balmer series) and quasiperiodic pulsations

Yu.A. Kupryakov[1,2], K.V. Bychkov[2], O.M. Belova[2], A.B. Gorshkov[2], M. Bárta[1]

[1] Astronomical Institute of the Czech Academy of Sciences, Fričova 298, 25165 Ondřejov, Czech Republic
e-mail: kupry@asu.cas.cz

[2] Sternberg Astronomical Institute, Moscow State University, Universitetsky pr. 13, Moscow 119234, Russia

ABSTRACT

This work aims to study the behavior of radiation intensity curves in the $H\epsilon$, $H\beta$, and $H\alpha$ lines during the development of a flare and compare the results with calculated values. Observations were carried out with the horizontal solar telescope HSFA-2 (Ondřejov Observatory). The 2013-05-17 M3.2 flare in the NOAA AR 11748 was selected for processing, and the absolute values of fluxes in the spectral lines were determined. It is shown that the model of heating of the chromospheric gas by the flow of magnetohydrodynamic waves from the convective zone and its ionization and excitation by the flow of suprathermal particles from the corona satisfies the observations. Calculations are performed in hydrogen lines, taking into account the main processes that determine the radiation of gas, opaque in spectral lines. The flat decrement of the Balmer series indicates the inhomogeneity of the radiating region along the vertical. The search for quasiperiodic pulsations showed that in this flare they were found only in the $H\alpha$ line with a significance level of 95%. They are absent in other spectral ranges.

Key words: spectral lines, solar flares, chromospheric radiation, quasiperiodic pulsations

1 Introduction

The recent discovery of thin magnetic loops in the chromosphere with a temperature of about a million degrees (Haisheng et al., 2012), with hot dense plasma ejected from their bases, indicates the possibility of plasma heating and particle acceleration directly in the chromosphere. The detected powerful terahertz radiation from active regions may be an additional factor for the occurrence of sporadic processes of particle acceleration and plasma heating in the chromosphere (Kaufmann et al., 1986). The analysis in Zaitsev et al. (2013) shows that for terahertz radiation, the plasma mechanism is the most probable, realized in dense compact and very hot sources located at chromospheric levels with plasma concentrations on the order of 10^{14}–10^{15} cm^{-3}, which is also confirmed in Morgacheva et al. (2019) when analyzing the millimeter radiation of a solar flare on April 2, 2017, observed with the RT-7.5 radio telescope of the Bauman Moscow State Technical University. The results show that terahertz radiation is formed in a thin chromospheric layer about 10 km thick with a plasma temperature of $\sim 10^5$ K. Using the example of solar flare SOL 2013-05-17, we tried to determine the mechanism of chromospheric heating.

2 Observations and data processing

All spectral observations were obtained by us at the Ondřejov Observatory of the Czech Academy of Sciences using the Multichannel Flare Spectrograph (MFS, 230 mm/13.5 m) and the Horizontal-Sonnen-Forschungs-Anlage spectrograph (HSFA-2, 500 mm/35 m). We used X-ray flare observation and microwave radiation data (Radio Solar Telescope Network, RSTN), as well as data from the RT3 radio telescope at 3.0 GHz (Ondřejov Observatory) and the Geostationary Operational Environmental Satellite (GOES).

We selected the M3.2 class flare on May 17, 2013, in the NOAA AR 11748 (N12 E22). The onset of the flare is at 08:43, its peak at 08:57, and the end at 09:19 UT.

Figure 1b shows the X-ray emission during the flare; the vertical lines correspond to the following data processing moments: 8:45:09; 8:46:43; 8:48:28; 8:56:33; 8:57:23; 8:58:52; 9:00:52 UT. Figure 2 shows the chromospheric region on the spectrograph slit (1). The vertical line corresponds to the slit position. The figure also shows the spectra of CaII H + Hϵ (2), Hβ (3), and Hα (4).

After data reduction, line profiles in the active and quiet chromospheric regions were obtained (Fig. 3) and radiation flux values were determined. The shaded area corresponds to the area of fluxes in the flare. Table 1 presents the measured flux values in the spectral lines at the selected moments.
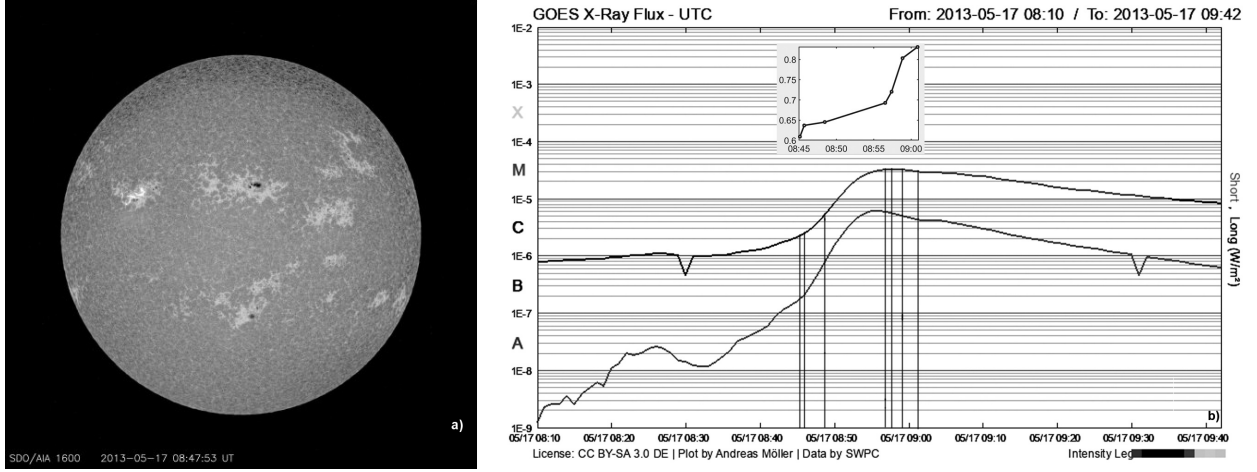
Fig. 1. a) Filtergram in the 1600 Å line at 08:57 UT from the Solar Dynamics Observatory (SDO, Pesnell et al., 2012). b) Change in the X-ray flux during the flare (GOES-15 data); the values selected for processing are indicated. The upper window of the figure shows the evolution of the half-width of the Hα line, Å. A delay of about 12 min is noted between the beginning of increasing the Hα half-width and the X-ray flux.
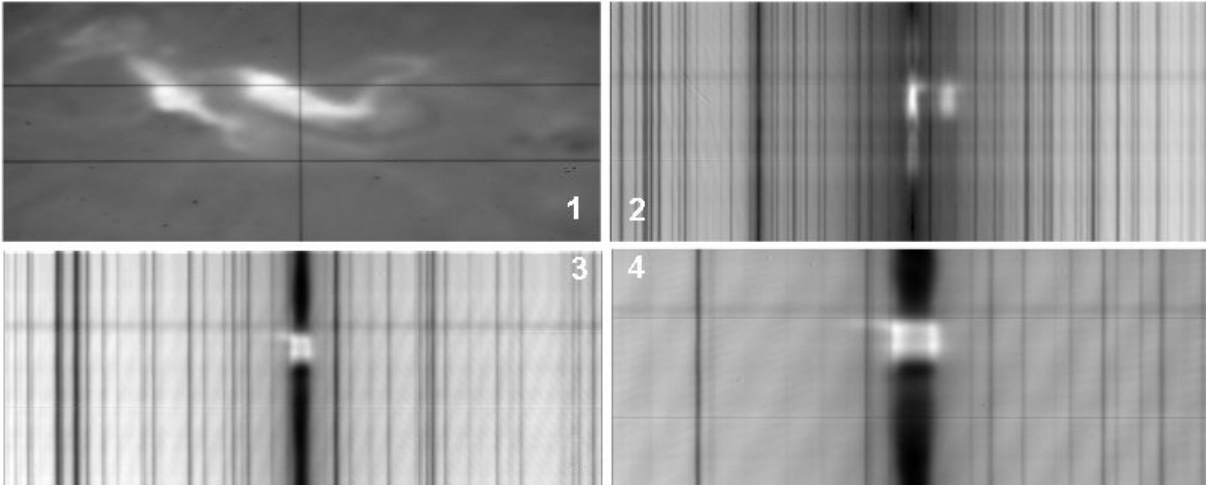
Fig. 2. Image of the chromosphere in the Hα line on the spectrograph slit (1) and the spectra of CaII H + Hε (2), Hβ (3), and Hα (4) at 08:56:33 UT.

Table 1. Integral flux values in the lines, in erg/cm^2/s, for each moment of time.

Time	08:45:09	08:46:43	08:48:28	08:56:33	08:57:23	08:58:52	09:00:52
Hε	1.18e + 7	1.57e + 7	2.92e + 7	3.76e + 7	3.58e + 7	3.64e + 7	2.54e + 7
Hβ	7.08e + 6	1.19e + 7	2.51e + 7	3.50e + 7	3.19e + 7	3.04e + 7	2.02e + 7
Hα	2.98e + 6	6.05e + 6	1.31e + 7	2.11e + 7	1.94e + 7	1.74e + 7	9.41e + 6

3 Model and method for calculating hydrogen lines

We adopted a model of a gas that is transparent in the continuous spectrum of the optical range but undergoing possible self-absorption at the frequencies of spectral lines. The populations of discrete levels and the ionization state of chemical elements, necessary for calculating the linear radiation flux, were determined by solving the balance equations written

for 12 levels of the hydrogen atom. Typical processes for the objects under consideration (for example, Biberman et al., 1982) were taken into account: bound-free, free-bound, and bound-bound collisional and radiative transitions. A detailed description of the algorithm used is given in Belova, Bychkov (2017). Atomic data for hydrogen are taken from Johnson (1972). The radiation transfer calculation was performed within the framework of the Sobolev–Holstein–Biberman photon escape probability model (Biberman, 1947; Holstein,
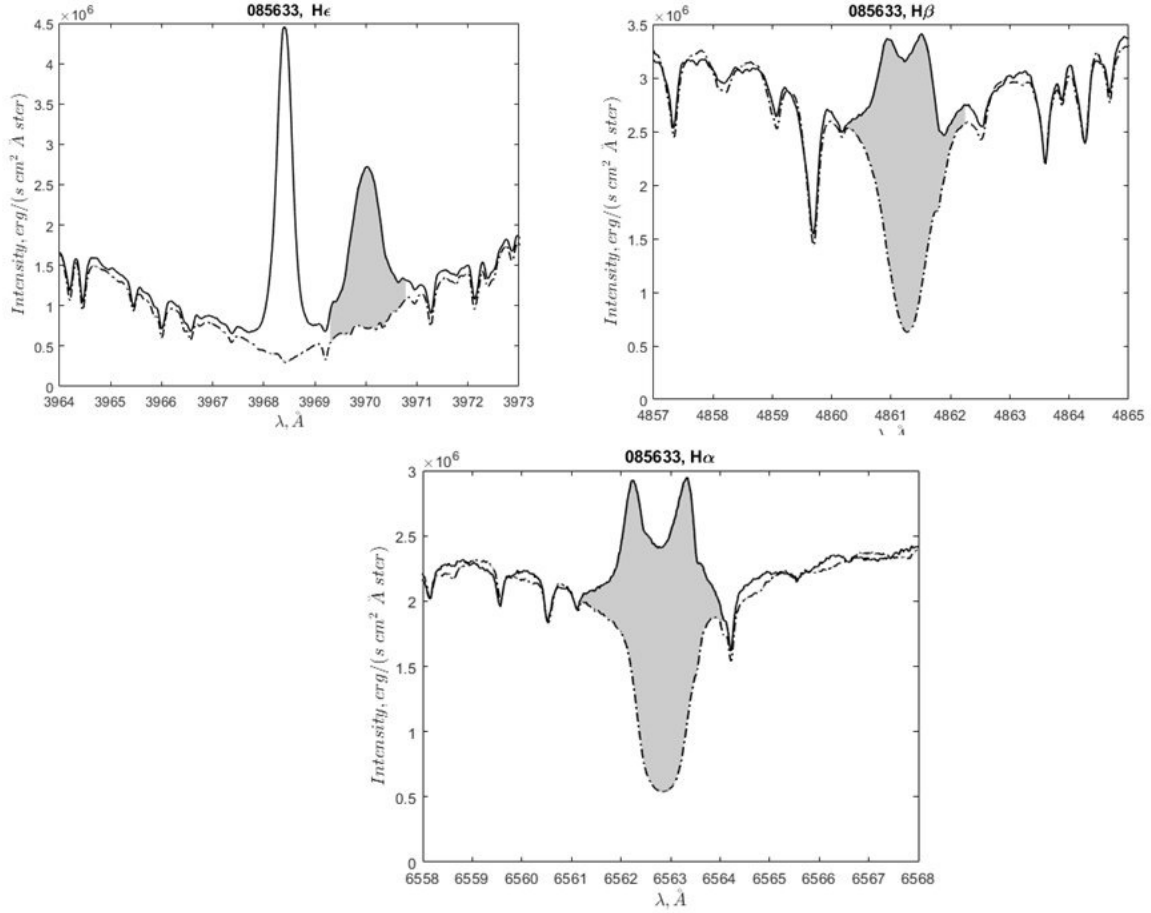
Fig. 3. Spectral line profiles in the active (solid lines) and the quiet (dash-dotted lines) chromosphere. The shaded part corresponds to a flux in the line. The position of the Hε line is indicated on the H CaII profile.

1947, 1951); for the hydrogen atom, we applied a convolution of the Doppler and Holtsmark contours. The photospheric radiation in the optical range is simulated by a black body model with a temperature of 5500 K. The temperature and density of the layers were selected so that the theoretical radiation fluxes in the lines corresponded to the observed ones.

Our calculations within the framework of the processes taken into account above showed that the observed fluxes in the lines cannot be explained by the model of an isolated homogeneous layer for any combination of temperature, density, and thickness of the gas layer. Therefore, we performed the interpretation of all episodes under the assumption of an inhomogeneous gas. The inhomogeneity was simulated in the form of homogeneous layers with different values of thickness, density, and temperature, located one behind the other along the line of sight. Moreover, the near layer partially absorbs the radiation of the more distant one. The results for two gas layers are shown in Fig. 4, where the following values are given:

a) observed and calculated fluxes in erg/cm^2/sec for the Hα, Hβ, and Hε lines;
b) layer thickness in kilometers;
c) hydrogen concentration in cm^{-3};

d) electron temperature in Kelvin.

4 Quasiperiodic pulsations

Now let us turn to the issue of searching for quasiperiodic pulsations (QPPs) in this flare. In recent years, it has become clear that QPPs are an integral feature of solar flares, since almost all flares have QPPs. Moreover, it is now firmly established that QPPs often have several periods. Until now, it has not been possible to definitively determine the triggering mechanism or cause of QPPs (Van Doorsselaere et al., 2016).

Currently, there are two main classes of mechanisms that explain QPPs. The first class associates the observed pulsations with a direct impact of magnetohydrodynamic (MHD) waves, and the second one with a repetitive magnetic reconnection process (Kupriyanova et al., 2020). The mechanisms of the two classes often coexist and complement each other. We tried to find out what is observed in this case and in which spectral range it manifests itself. For processing, we selected data obtained in the optical, radio, and X-ray ranges. The technique for signal processing and determining the QPP periods is described in detail in Kupryakov et al. (2022).

The results are as follows:
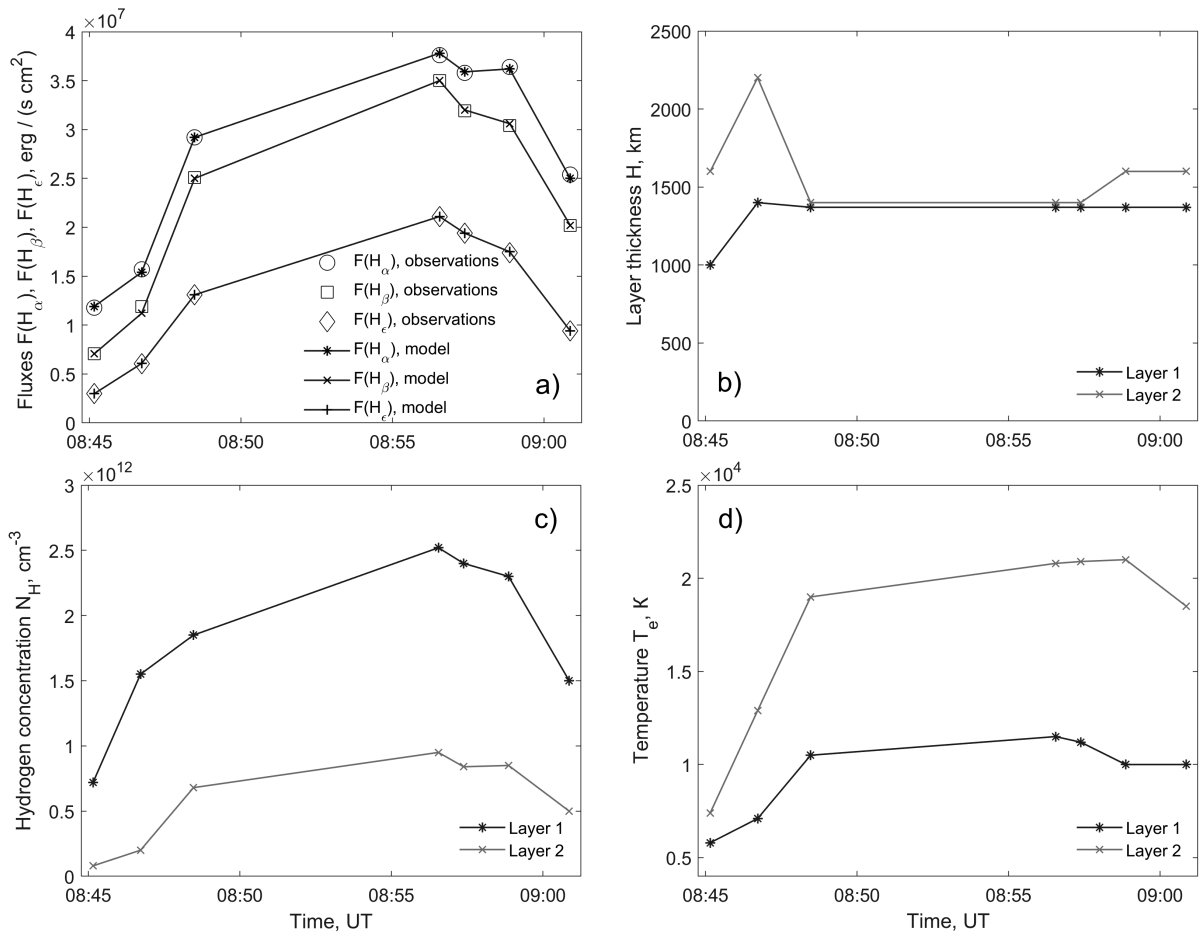
Fig. 4. Results of theoretical calculations of fluxes in the 2013-05-17 flare.
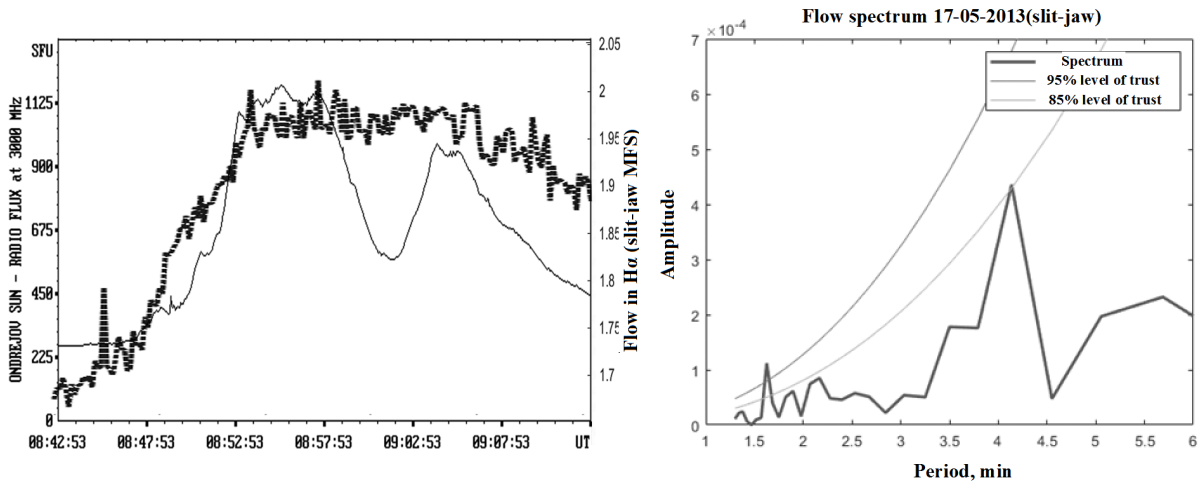
Fig. 5. a) Radiation intensity flux in the radio range at 3 GHz (solid line) and from chromospheric observations in the Hα line on the MFS slit-jaw image, with a series discreteness of 10 s (dashed line). b) Spectrum of the Hα flux.

a) in the chromospheric radiation flux in the Hα line, peaks with a period of 1.625 min (95 % confidence level) and 4.136 min (85 % confidence level) were revealed, see Fig. 5a;

b) in the microwave radiation data (Radio Solar Telescope Network, RSTN), no pulsations were detected, only noise (although the data are good) – i.e., this is a reliable result, although negative;

c) in the 3.0 GHz radio data flux, with the presence of a long continuous data series (Fig. 5c), it was also not possible to detect pulsations.

The same statement can be made for the RHESSI and FERMI/GBM data. Although in our previous works using this method (Kupryakov et al., 2022), we found a whole spectrum of similar pulsations in other flares. This fact may indicate that in this case, we have a flare with plasma heating by MHD waves rather than with the reconnection of magnetic tubes.

5 Conclusions

1. The flare onset corresponded to 08:35 UT in X-rays, 08:45 UT in the optical range, and 8:46 UT in the 3 GHz radio range. We also observe a 12-minute delay between the start of the X-ray flux increase and the start of the Hα half-width (FWHM) increase, as well as the enhancement of microwaves. This suggests that we necessarily encounter the effect of the gas-dynamic process of chromospheric heating. This process may be associated with an increase in the volume of heated plasma, evaporation, or plasma motion (Kotrč et al., 2013). The effect of a very close correlation between the Hα FWHM and microwaves undoubtedly corresponds to the classical theory of flare physics.
2. The presented fluxes during the flare development indicate a strong inhomogeneity of the radiating gas. For example, for the moment 8:46:43 UT:
   a) the Hϵ line, which is strong relative to Hβ (Hϵ/Hβ = 0.53), is emitted by dense ($N = 1.55\,10^{12} \mathrm{cm}^{-3}$) and cold ($T_e$ = 7100 K) regions with a thickness H of about 1400 km;
   b) the flat Balmer decrement (Hα/Hβ=1.37) gives a region with a size of 2200 km; its temperature is T_e = 12900 K and the concentration is $N = 2.0\,10^{11} \mathrm{cm}^{-3}$.
3. The thickness of layer 1 does not change during the flare development, while the thickness of layer 2 increases by the end of the flare.
4. The hydrogen concentration and temperature change symmetrically in the first and second layers during the flare.

5. Surprisingly, QPPs were detected only in the Hα emission. In all other ranges, their manifestation was not detected despite long and continuous observation series.

References

Belova O.M., Bychkov K.V., 2017. Astrophysics, vol. 60, pp. 111–117.

Belova O.M., Bychkov K.V., 2018. Astrophysics, vol. 61, pp. 224–240.

Biberman L.M., 1947. ZhETF, vol. 17, p. 416. (In Russ.)

Biberman L.M., Vorob'ev V.S., Yakubov I.T., 1982. Kinetics of Nonequilibrium Low-Temperature Plasmas, M.: Nauka. (In Russ.)

Haisheng Ji, Wenda Cao, Goode P.R., 2012. Astrophys. J., vol. 750, p. L25.

Holstein T., 1947. Phys. Rev., vol. 72, pp. 1212–1233.

Holstein T., 1951. Phys. Rev., vol. 83, pp. 1159–1168.

Johnson L.C., 1972. Astrophys. J., vol. 174, pp. 227–236.

Kaufmann P., Correa E., Costa J.E.R., Zodi Vaz A.M., 1986. Astron. Astrophys., vol. 157, p. 11.

Kotrč P., Bárta M., Schwartz P., Kupryakov Yu.A., Kashapova L.K., Karlický M., 2013. Solar Phys., vol. 284, pp. 447–466.

Kupriyanova E.G., Kolotkov D.Yu., Nakariakov V.M., Kaufman A.S., 2020. Solar-Terrestrial Physics, vol. 6, pp. 3–23.

Kupryakov Yu., Gorshkov A., Kashapova L., Barta M., 2022. Izv. Krymsk. Astrofiz. Obs., vol. 118, no. 3, pp. 58–62. (In Russ.)

Morgachev A.S., Tsap Yu.T., Smirnova V.V., Motorina G.G., 2019. Geomagnetism and Aeronomy, vol. 59, pp. 1114–1120.

Pesnell W.D., Thompson B.J., Chamberlin P.C., 2012. Solar Phys., vol. 275, pp. 3–15.

Van Doorsselaere T., Kupriyanova E.G., Yuan D., 2016. Solar Phys., vol. 291, pp. 3143–3164.

Zaitsev V.V., Stepanov A.V., Mel'nikov V.F., 2013. Pis'ma v Astron. zhurn., vol. 39, pp. 1–11. (In Russ.)